

UNDULAR JUMP FORMATIONS IN VERY LARGE CHANNELS

M. Ben Meftah¹, F. De Serio¹, M. Mossa², A. Pollio²

- (1) Dipartimento di Ingegneria delle Acque e di Chimica, Politecnico di Bari – Bari (IT)
e-mail: mbenme@poliba.it, f.deserio@poliba.it
- (2) Dipartimento di Ingegneria dell'Ambiente e per lo Sviluppo Sostenibile, Politecnico di Bari – Bari (IT)
e-mail: m.mossa@poliba.it, a.pollo@poliba.it

Keywords: Hydraulic jump, free surface current, shockwave.

ABSTRACT

In this paper, undular hydraulic jumps in very large channel (channel width equal to 4.0 m) for low Reynolds number have been investigated. Jumps with very high aspect ratios are very rare in literature, and, therefore, experimental works are necessary. The main aims are (i) analyzing the lateral shock wave in order to verify the experimental validity of the shock wave theory in very large channel, (ii) analyzing the flow conditions of undular jumps in very large channels. The main results are the following: (i) the presence of well developed lateral shock wave similar to those of oblique jumps were observed; (ii) the comparison of the experimental results and the theoretical ones show that the classical shock wave theory is confirmed, taking into account the experimental errors; (iii) the literature law of the wave height of first wave crest was confirmed also in the case of very large channels.

1 INTRODUCTION

The undular jump is formed for low supercritical inflow Froude numbers, and is characterized by undulations of the water surface without a surface roller (Chow, 1959). The formation of undular jumps can be seen in a flood flow or flow below a sluice gate or a weir, and undulations might cause bank erosion (Reinauer & Hager, 1995). The characteristics of undular jumps are significant for the design and management of hydraulic structures. Because of the formation of undulations without a surface roller, undular jumps might be useful for planning water sports and recreational activities such as canoeing and rafting in rivers (Ohtsu et al., 2001).

Chanson & Montes (1995) performed experiments on undular hydraulic jumps with fully developed turbulent shear flows, with rectangular channel width of 0.25 m, indicating five types of undular jumps. Furthermore, the Authors observed that the lateral shock waves (or “Mach” waves) are connected with the existence of sidewall boundary layers. The sidewall boundary layers retard the fluid near the wall and force the apparition of critical conditions there, sooner than on the channel centreline. Chanson & Montes (1995) observed also that their experimental data are in opposition with the classical theory of shock waves in supercritical flow (Ippen, 1951), which predicts a reduction of the angle between lateral shock waves and sidewalls with increasing Froude numbers. Reinauer & Hager (1996) analyzed the effect of air-flow on shockwave applying the shock equations of Ippen. Ohtsu et al. (1997) observed that fundamental factors governing the undular jump are generally the supercritical inflow Froude number, the inflow conditions (the state of the boundary layer development), the aspect ratio, the Reynolds number, and also the ratio between the longitudinal length from the toe of the lateral shock wave to the cross point of the shock wave and the longitudinal length from the toe of the shock wave to the first wave crest.

Montes & Chanson (1998) observed that shock waves first form just downstream of the beginning of the undular jump. The Authors observed that the formation of the shock wave is in itself paradoxical. In transonic flow, shock waves' existence is associated with the existence of a body with surface discontinuities; in hydraulics with changes of alignment of the channel walls, which were not met in their study. Montes & Chanson (1998) advanced “the idea that the shock waves formed due to the rapid growth of the

boundary layer on the side walls caused by the adverse pressure gradient at the beginning of the jump. The supercritical flow regards the solid boundary of the side wall as being displaced inward by the lateral boundary layer, and when the side-wall boundary layer thickens appreciably due to the adverse pressure gradients and eventually separates from wall, the shock wave starts." Nevertheless the Authors observed a divergence of their experimental results from the shock wave formation theory ascribed to the interaction between the shock wave and the lateral boundary layer. *Montes & Chanson (1998)* observed also that the adverse pressure gradient on the boundary layer increases with the Froude number because of the increased depth ratio between the upstream position and the first crest position. The lateral boundary layer consequently thickens and eventually separates near the point of shock wave formation, enabling to conjecture that an equilibrium is reached, in which the angle between lateral shock waves and side walls remains constant with increasing inflow Froude number.

Ohtsu et al. (2001) performed experiments with rectangular channel widths between 80 cm to 105 cm, presenting the upper limit of the inflow Froude number for undular jumps formations. The Authors observed that the formation of undular jumps depends not only on the inflow Froude number, but on the boundary layer development at the toe of the jump under conditions in which the effects of the aspect ratio and the Reynolds number on the flow condition are negligible. *Ohtsu et al. (2001)* proposed also a relation between the wave height of the first wave crest and the inflow Froude number.

Ohtsu et al. (2003) investigated the flow conditions of undular jumps with fully developed inflow in rectangular channels 10.5 cm to 165 cm wide. The Authors concluded that the flow conditions of undular jumps can be classified based on the intersection of lateral shock waves and the inflow Froude number, observing also (i) the importance of the Reynolds number and (ii) the increasing of the angle of lateral shock waves to sidewall with the increase of the Froude number, in contrast with the classical shock wave theory.

In this paper, undular hydraulic jumps in very large channel (channel width equal to 4.0 m) for low Reynolds number are investigated. Jumps with very high aspect ratios are very rare in literature, and, therefore, experimental works are necessary. The main aims are (i) analyzing the lateral shock wave in order to verify the experimental validity of the shock wave theory in very large channel, (ii) analyzing the flow conditions of undular jumps in very large channels.

2 THEORETICAL BACKGROUND

As shown by *Ippen (1951)*, see also *Chow (1959)*, when a supercritical flow is deflected inward to the course of the flow by a vertical boundary (Fig. 1), the depth of the flow h_1 will increase abruptly to a depth h_2 along a wavefront CD which extends out from the point of boundary discontinuity at a wave angle β that depends in magnitude on the angle of deflection θ of the boundary. This phenomenon resembles a normal hydraulic jump but with the change in depth occurring along an oblique front. Therefore, it may be called an oblique hydraulic jump. When $\theta=0$, oblique jump becomes the familiar hydraulic jump in which the wavefront is normal to the flow direction, i.e. $\beta=90^\circ$.

Referring to the relationship of velocity vectors before the jump in Fig. 1, the velocity normal to the wavefront is $V_{n1}=V_1 \sin\beta$, where V_1 is the velocity of the flow before the jump. The Froude number normal to the wavefront before the jump is

$$F_{n1} = \frac{V_{n1}}{\sqrt{gh_1}} = \frac{V_1 \sin \beta}{\sqrt{gh_1}} = F_1 \sin \beta \quad (1)$$

Considering a section A-A normal to the wavefront, it is seen that a normal hydraulic jump occurs in this section and that the following equation

$$\frac{h_2}{h_1} = \frac{1}{2} \left(\sqrt{1 + 8F_1^2} - 1 \right) \quad (2)$$

can be applied.

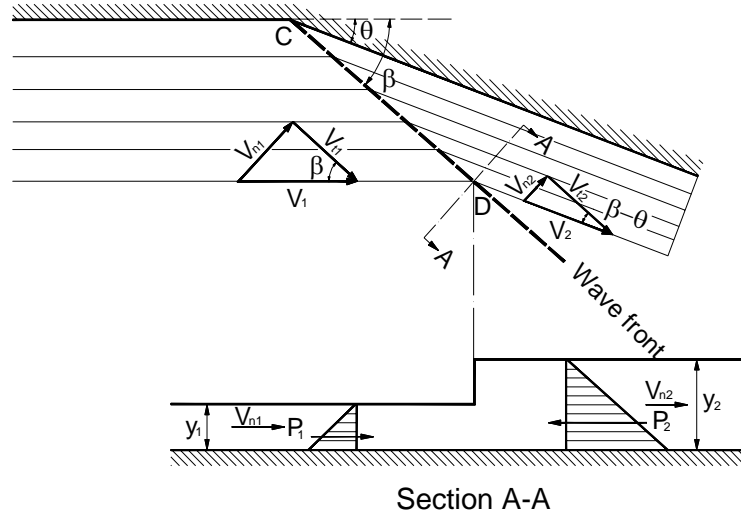


Figure 1. Sketch of shock a wave at a wall deflection.

Substituting eq. (1) for F_1 in eq. (2), the ratio of the sequent to initial depth is

$$\frac{h_2}{h_1} = \frac{1}{2} \left(\sqrt{1 + 8F_1^2 \sin^2 \beta} - 1 \right) \quad (3)$$

This is the equation that represents the condition for an oblique hydraulic jump to take place.

Referring to Fig. 1, the tangential velocities before and after the jump are $V_{t1} = V_{n1} / \tan \beta$ and $V_{t2} = V_{n2} / \tan(\beta - \theta)$. Since no momentum change takes place parallel to the wavefront, these two velocities should be equal, or

$$\frac{V_{n1}}{V_{n2}} = \frac{\tan \beta}{\tan(\beta - \theta)} \quad (4)$$

It is possible to write the continuity equation and the momentum equation for a unit length of wave crossing a flow of depth h_1 and velocity V_1 at an angle β as follows:

$$h_1 V_{n1} = h_2 V_{n2} \quad (5)$$

and

$$\frac{\gamma h_1^2}{2} + \frac{\gamma}{g} h_1 V_{n1}^2 = \frac{\gamma h_2^2}{2} + \frac{\gamma}{g} h_2 V_{n2}^2 \quad (6)$$

From eqs. (5) and (6) the expression for the normal component V_{n1} is obtained in terms of the depths h_1 and h_2

$$V_{n1} = \sqrt{gh_1} \sqrt{\frac{h_2}{h_1} \frac{1}{2} \left(1 + \frac{h_2}{h_1} \right)} \quad (7)$$

If $V_{n1} = V_1$, the wave front assumes a position at a right angle to the flow, and becomes the familiar hydraulic jump.

The relation between V_1 and V_{n1} may best be given by the ratio V_{n1}/V_1 from the vector diagram as $\sin\beta = V_{n1}/V_1$. Substituting for V_{n1} in eq. (7) the equivalent $V_1 \sin\beta$ and solving for $\sin\beta$, the expression

$$\sin \beta = \frac{\sqrt{gh_1}}{V_1} \sqrt{\frac{h_2}{h_1} \frac{1}{2} \left(1 + \frac{h_2}{h_1}\right)} = \frac{1}{F_1} \sqrt{\frac{h_2}{h_1} \frac{1}{2} \left(1 + \frac{h_2}{h_1}\right)} \quad (8)$$

is obtained. By eq. (5), eq. (4) can be written

$$\frac{h_1}{h_2} = \frac{\tan \beta}{\tan(\beta - \theta)} \quad (9)$$

Eliminating h_1/h_2 from eqs. (3) and (9), a relationship involving F_1 , θ , and β is obtained:

$$\tan \theta = \frac{\tan \beta \left(\sqrt{1 + 8F_1^2 \sin^2 \beta} - 3 \right)}{2 \tan^2 \beta + \sqrt{1 + 8F_1^2 \sin^2 \beta} - 1}. \quad (10)$$

According to *Ippen & Harleman (1956)*, if $F_{n1} < 1.7$, the oblique jump becomes undular.

3 EXPERIMENTAL SET-UP AND RUNS

The experiments were carried out at the Technical University of Bari, Italy in the Coastal Engineering Laboratory (L.I.C.) of the Water Engineering and Chemistry Department. The system consisted of a rectangular steel channel (Fig. 2), with base and the lateral walls in transparent glass material (Saint Gobain) of thickness 15 mm, connected and sealed internally with silicone rubber watertight and also able to prevent thermal dilatation. The base covered a surface of 15 m by 4 m and it was 0.96 m distant from the floor, whereas the height of the walls, and so the depth of the channel, was 0.4 m. To create a current inside the channel, a closed hydraulic circuit was constructed. The water was supplied from a downstream big metallic tank by a Flygt centrifugal electro-pump, which sucked the water into a steel pipe with diameter 200 mm and then discharged the same water into the upstream steel tank. Into the upstream tank a side-channel spillway with adjustable height was fitted, being made from different plates mounted together. The water that overflowed was directed into a pipe like the one for the water supply and parallel to it, with a 250 mm diameter and finally discharged into the tank downstream of the channel. Two different electromagnetic flow meters were mounted on the two parallel pipes described above in order to measure the flow rate in the channel as the difference of the two discharge measurements. The upstream gate was used to define the upstream current, whereas the downstream gate was fully opened.

For the measurement of the velocity the Nortek ADV system was used, together with CollectV software for the data acquisition and ExploreV software for the data analysis, all of them products of Nortek.

Water height was measured using an ultrasonic measuring system UltraLab ULS 2001300 by General Acoustics, characterized by a resolution of 0.18 mm.

Four tests were analyzed, characterized by a channel discharge of 0.1 m³/s. Table 1 shows the inflow current type, the jump type, h_1 =average height of the inflow current, h_{max} =wave height of the first wave crest in the undular jump in the centreline longitudinal section, V_0 = average inflow current velocity, F_0 =average Froude number of the inflow current, T =water temperature, ν =water kinematic viscosity, $Re = V_0 h_1 / \nu$ =Reynolds number. Since in each vertical profile of the inflow current it was not possible to measure the velocity in more than one point and, therefore, it was not possible to measure a vertical velocity profile, the inflow current type was defined following the criteria of *Leutheusser & Alemu (1979)*. They observed that the existence of fully developed supercritical turbulent flow depends mainly on the Reynolds number of flow, but prevails for all values of $x/b \geq \lambda/b \geq 200$, where x =longitudinal coordinate with origin in the plane of the vena contracta, λ =length of flow development, and b =opening of sluice gate.

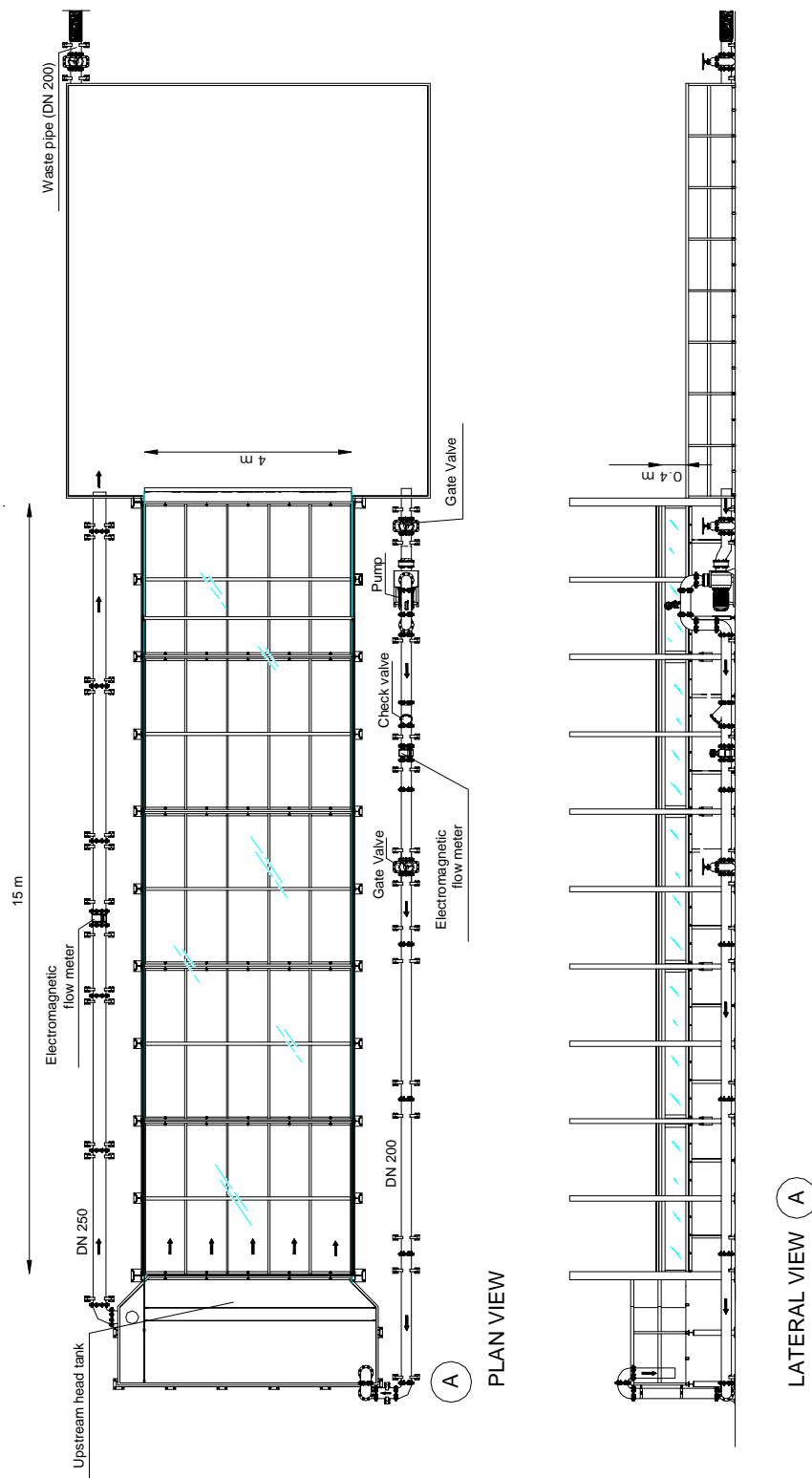


Figure 2. Sketch of the channel used for the experiments.

Test	Inflow current	Jump type	h_1 [m]	h_{max} [m]	V_0 [m/s]	F_0	T [°C]	v [m ² /s]	Re
1	Fully developed	Undular breaking	0.020	0.076	1.25	2.82	8.30	1.413E-06	1.769E+04
2	Undeveloped	Undular breaking	0.024	0.080	1.04	2.15	8.88	1.385E-06	1.805E+04
3	Undeveloped	Undular breaking	0.025	0.078	1.00	2.02	9.80	1.342E-06	1.863E+04
4	Undeveloped	Undular breaking	0.026	0.090	0.96	1.90	10.06	1.331E-06	1.879E+04

Table 1. Experimental conditions.

In the present study, since the channel is very large, the hydraulic jump front is trapezoidal, as shown in the sketch of Fig. 3, with presence of lateral shock waves. In all hydraulic jumps analyzed an eddy and circulation pattern is present due to the lateral flow separation. The separation surfaces shown in Fig. 3 by dashed lines act as solid boundaries within which the flow has the characteristics similar to oblique jump, except in the channel center zone where the hydraulic jump front is normal to the inflow velocity. This type of flow feature is analogous to than analyzed by *Carling* (1995), and by *Rouse et al.* (1951) for the case of channel expansion in supercritical flow.

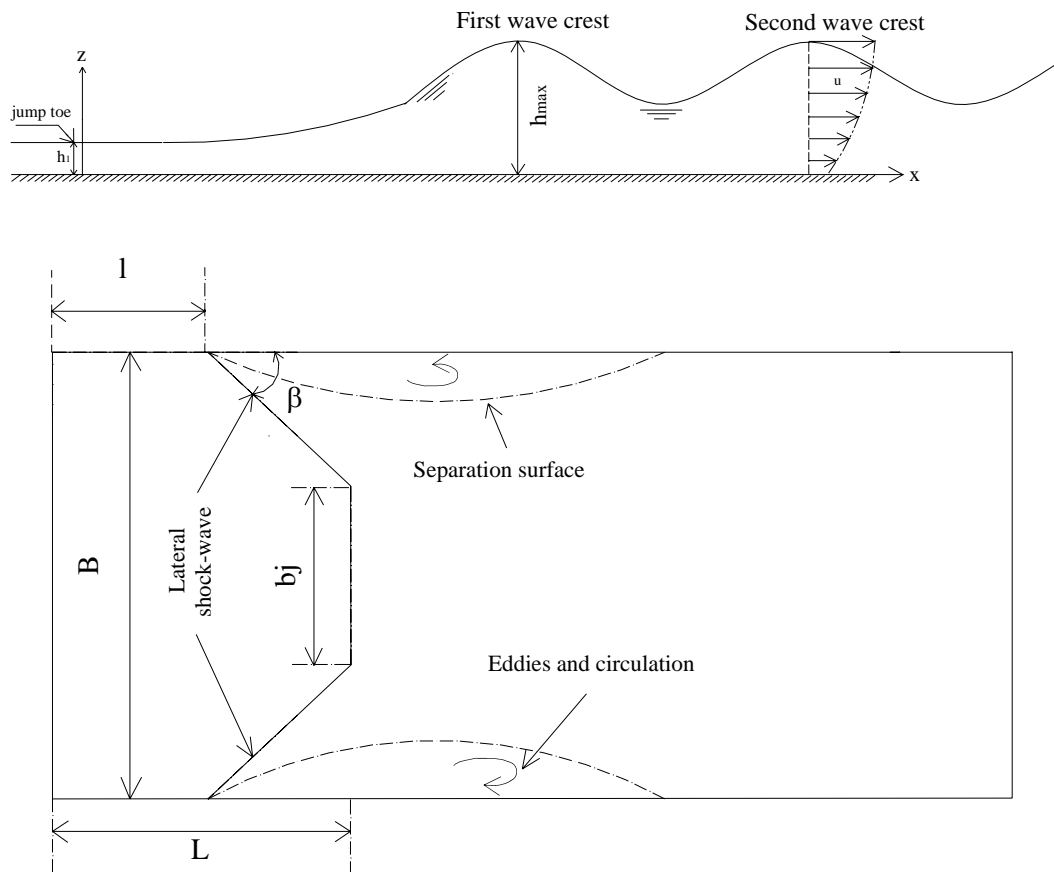
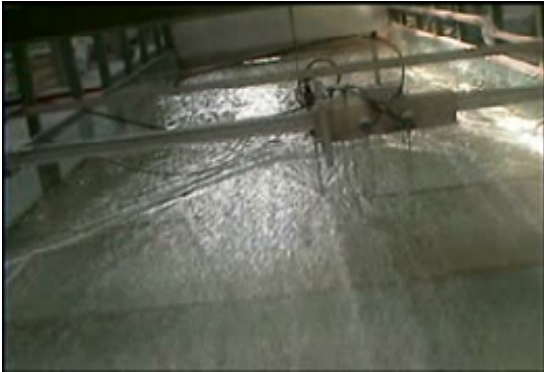


Figure 3. Definition sketch of the undular hydraulic jump.

Test 1	 A photograph showing a hydraulic jump in a channel. The water surface is relatively smooth upstream and becomes turbulent and frothy at the jump. The front of the jump is trapezoidal in shape.	 A close-up photograph of the hydraulic jump, showing lateral shock waves and a circulation zone. The water is highly turbulent and frothy.
Test 2	 A photograph showing a hydraulic jump with a trapezoidal front and small waves on the surface. The water is turbulent and frothy.	 A close-up photograph of the hydraulic jump, showing lateral shock waves and a circulation zone. The water is highly turbulent and frothy.
Test 3	 A photograph showing a hydraulic jump with a trapezoidal front and small waves on the surface. The water is turbulent and frothy.	 A close-up photograph of the hydraulic jump, showing lateral shock waves and a circulation zone. The water is highly turbulent and frothy.

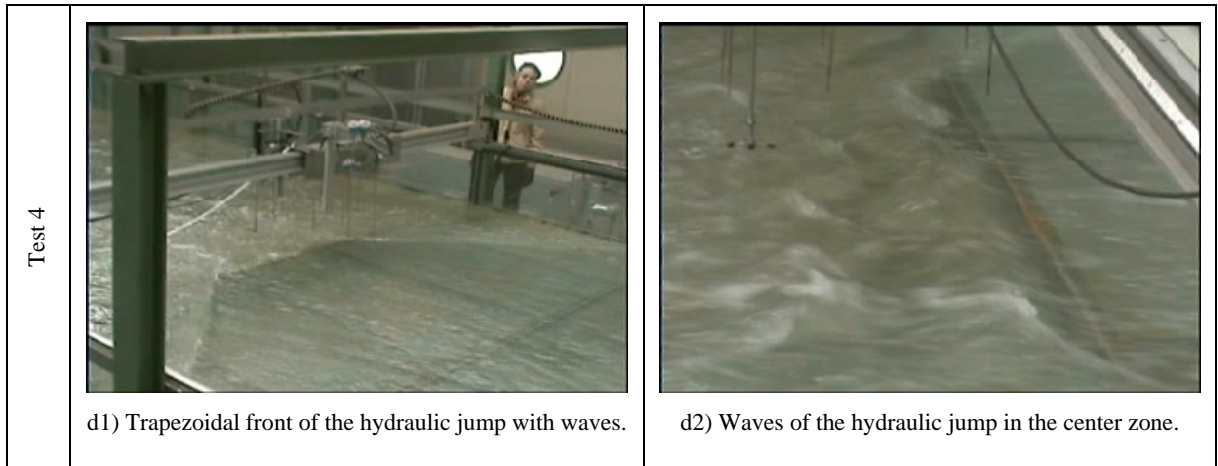


Figure 4. Photos of the analyzed hydraulic jumps.

4 TIME-AVERAGED VELOCITY AND SHOCK WAVE FRONT ANALYSIS

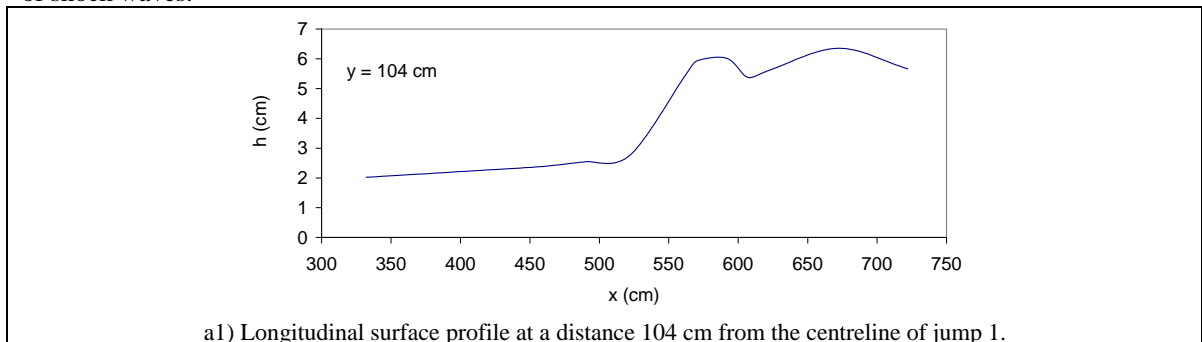
Table 2 shows the experimental parameters of Fig. 3, where L =longitudinal length from the upstream channel gate to the hydraulic jump front normal to the upstream current, l =longitudinal distance from the upstream channel gate to the toe of the shock wave, b_j =length of the hydraulic jump front normal to the upstream current, β =angle between the lateral shock wave and the channel side wall.

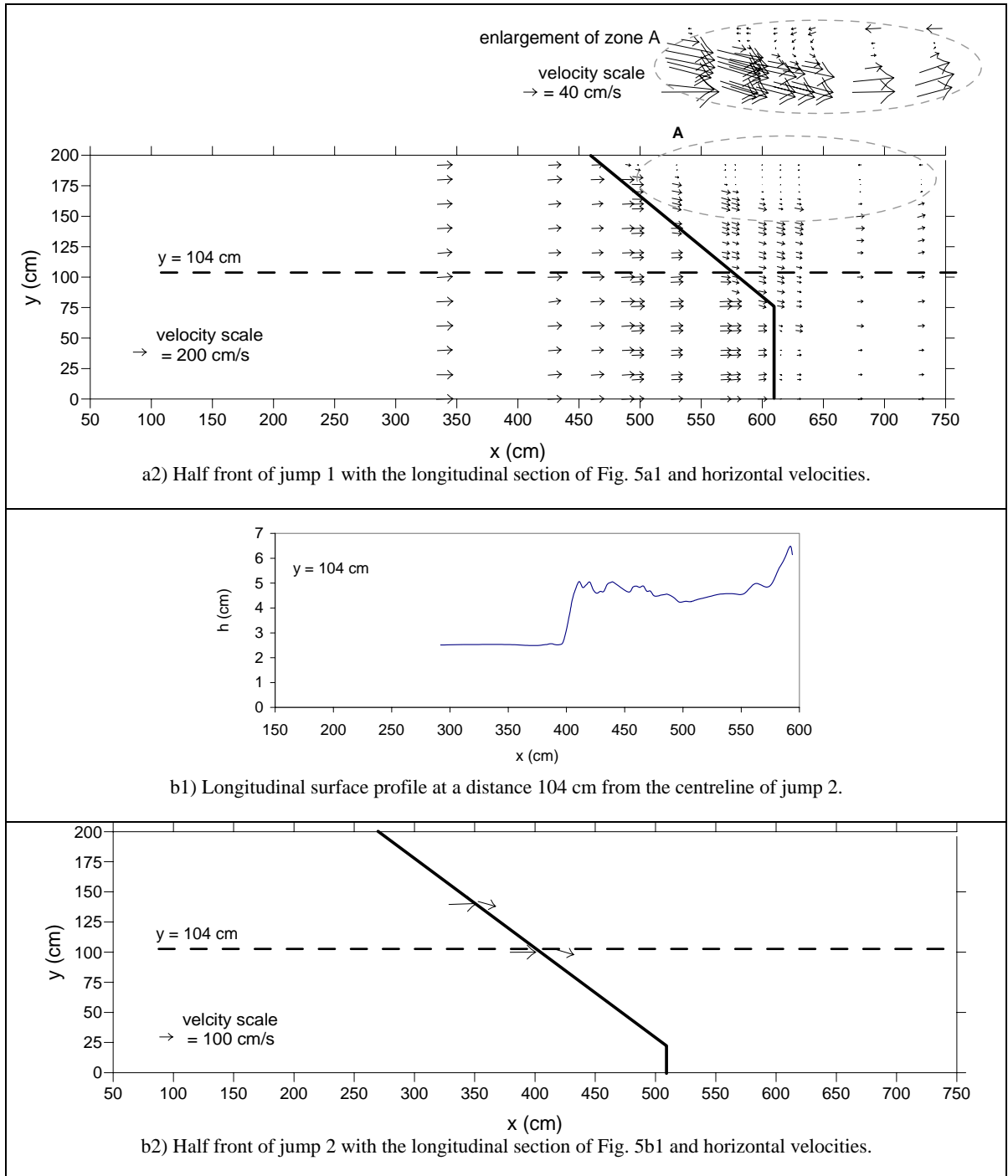
Test	L [m]	l [m]	b_j [m]	β [°]
1	6.1	4.58	1.52	39.21
2	5.1	2.70	0.36	37.17
3	3.9	2.05	0.50	43.41
4	3.1	1.65	0.96	46.35

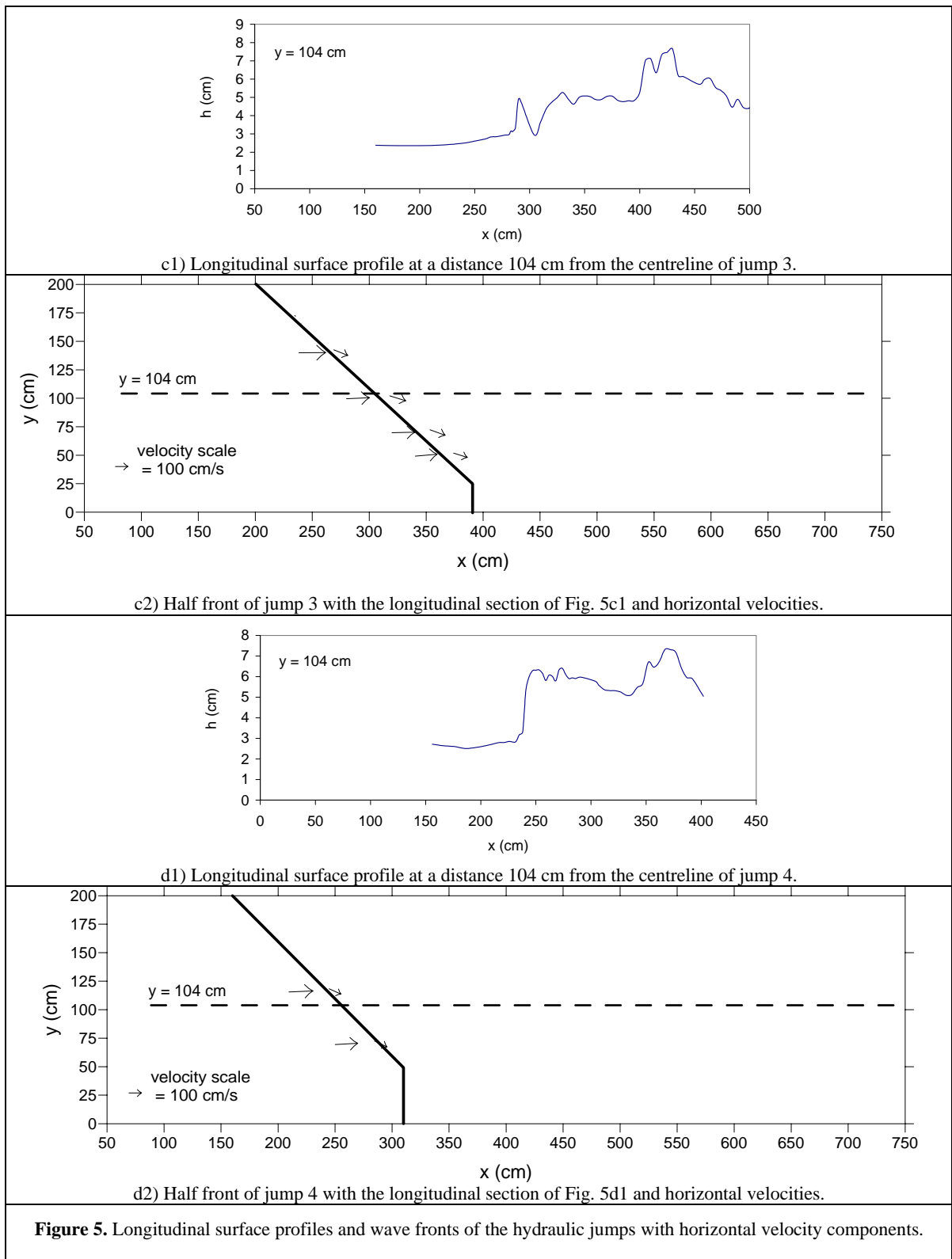
Table 2. Experimental parameters of the hydraulic jumps.

Figures 4 show two photos of each hydraulic jump analyzed in the present paper, highlighting the typical trapezoidal front and typical waves of undular jumps. In the photos the lateral shock waves with the circulation zones of Fig. 3 are also shown.

Figures 5 show the jump fronts for each hydraulic jump analyzed in the present paper. For the sake of brevity only a longitudinal surface profile crossing the lateral shock wave is also shown in Fig. 5. Generally, at the end of each longitudinal surface profile an intumescence is present, typical of the overlapping of shock waves.







Figures 5d1-5d4 show also the horizontal velocity components at 1 cm from the channel bed. In order to verify the validity of eqs. (4), (8) and (10) the velocity components were assessed immediately upstream and downstream of the shock wave front. Nevertheless, in order to show the circulation zone of Fig. 3, for test 1 the horizontal velocity components were assessed in a suitable number of measurement points.

Since the vertical velocity component was negligible and the flow was governed by the longitudinal and transversal flow velocity components, the flow was still bidimensional. Therefore, the use of a bidimensional ADV is suitable. In an effort to understand further the flow with the presence of hydraulic jump with a undular surface dynamics, spatial distribution of the average magnitude flow velocity vectors is presented and discussed in this section. The average flow velocity is the module of the time averaged longitudinal and transversal velocity components. According, certainly, to the quasi-symmetry of the flow relative to the longitudinal channel axis, measurements have been done in the plane ($x = 0$ to 8 m, $y = 0$ to 2 m). The velocity flow vectors in the plane ($x = 0$ to 8 m, $y = 0$ to -2 m) can be determined by symmetry relative to the longitudinal channel axis ($y = 0$).

Examining the magnitude and the orientation of the vectors it can be seen clearly the different characteristic patterns of the hydraulic jump and the flow around the wave front. The supercritical zone is individualized with the larger magnitude of the velocity vectors which are localized in the upstream side of the channel and form a trapezoidal shape. The trapezoidal shape is generated by both the symmetric reflected shock waves near the wall sides of the channel.

As shown always in Fig. 5, the flow downstream of the shock wave front is divided into three regions. A large flow band appears along the central axis of the channel and it is characterized by flow velocity vectors leaning toward the longitudinal direction. The two other flow regions are symmetric and are localized near the channel wall sides. They are characterized by a circulation pattern flow, where the flow velocity decreases dramatically and then the velocity vectors become opposite to the flow direction, as shown in the enlarged part of Fig. 5a2. The velocity vectors downstream of the shock wave front are characterized by a deflection of an angle θ , which, on the opposite of the oblique jump analyzed in par. 2, change from the channel wall to the zone with the front normal to the upstream velocity, where it is equal to zero.

Figure 6 shows the experimental validity of eq. (4), where all the parameters V_{n1} , V_{n2} , β , and θ are measured (see Figs. 5). The experimental results show that eq. (4) underestimates the values of V_{n1}/V_{n2} , even if, taking into account the experimental errors, its theoretical validity is sufficiently confirmed.

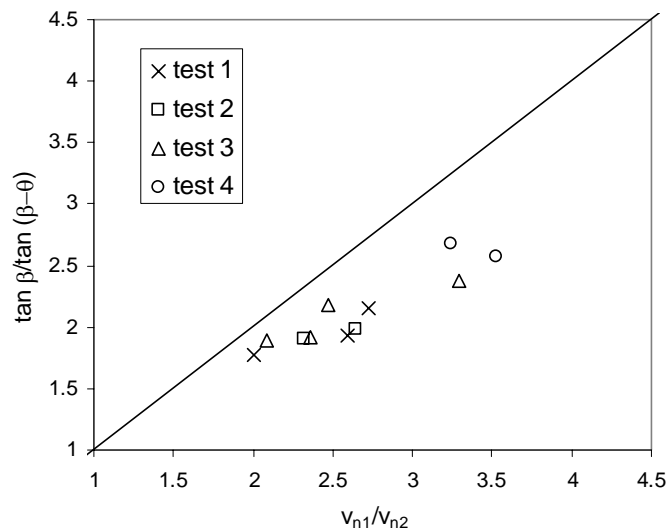


Figure 6. Experimental validity of eq. (4).

Figure 7 shows the experimental validity of eq. (8). In applying eq. (8), the values of h_2 were com-

puted by using eq. (5), where h_1 is shown in Table 1, V_1 are measured upstream of the lateral shock wave, and the local values of F_1 are those obtained with the aforementioned values of V_1 and h_1 . For each test and, therefore, for each value of $\sin \beta$ the average values of eq. (8) is shown. Taking into account the previous details, it is possible to conclude that the validity of eq. (8) has been sufficiently confirmed by the present experiments.

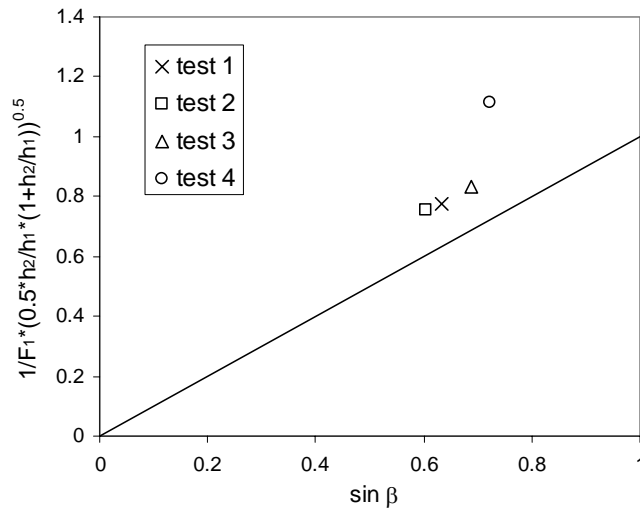


Figure 7. Experimental validity of eq. (8).

Figure 8 shows the experimental validity of eq. (10), where the values of θ and β are measured, and F_1 is that of Fig. 7. Taking into account the experimental errors it is possible to conclude that also eq. (10) is sufficiently confirmed.

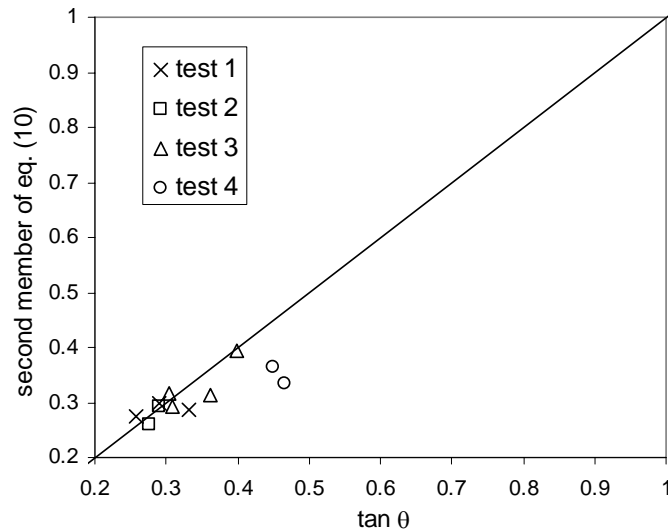


Figure 8. Experimental validity of eq. (10).

Therefore, the present experimental work enables to confirm the validity of the shock wave analysis proposed by *Ippen* (1951).

Figure 9 shows the wave height of the first wave crest as a function of the inflow Froude number. The

broken line and the continuous line show the theoretical wave heights for solitary wave

$$\frac{h_{\max}}{h_1} = F_0^2 \quad (11)$$

and that proposed by *Ohtsu et al.* (2001)

$$\frac{h_{\max}}{h_1} = 1.51F_0 - 0.35. \quad (12)$$

Following the procedure proposed by *Ohtsu et al.* (2001), the h_{\max} in the centreline and F_0 of Table 1 have been used. The experimental results confirm the validity of the law proposed by *Ohtsu et al.* (2001).

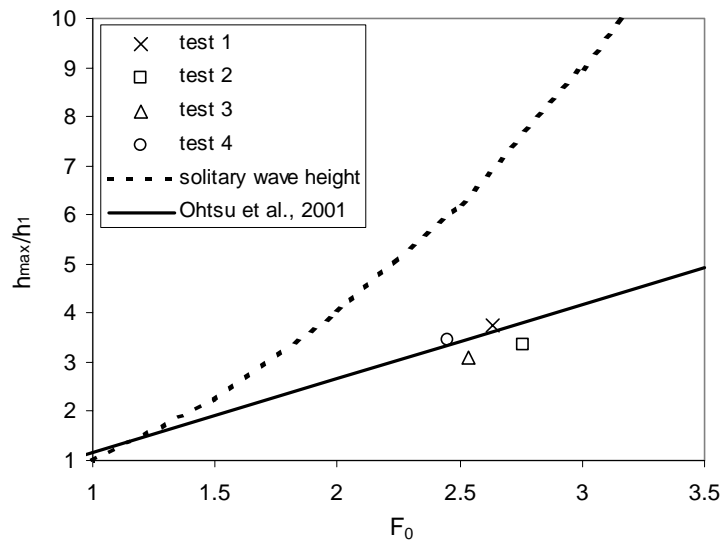


Figure 9. Wave height of first wave crest in undular jumps.

CONCLUSIONS

Undular breaking jumps were investigated in a horizontal rectangular very large channel, whose analysis is still very rare in literature. The main results may be summarized:

- (i) The presence of well developed lateral shock wave similar to those of oblique jumps were observed.
- (ii) The experimental validity of the classical shock wave theory were analyzed. The comparison of the experimental results and the theoretical ones show that the classical shock wave theory is confirmed, taking into account the experimental errors.
- (iii) The *Ohtsu et al.*'s law (2001) of the wave height of first wave crest was confirmed also in the case of very large channels.

NOTATIONS

The following symbols are used in this paper:

b = opening of sluice gate

b_j	=	length of the hydraulic jump front normal to the upstream current
F_0	=	Froude number characterizing the inflow current on the average
F_1	=	local Froude number in each measurement point upstream of the jump
F_{n1}	=	local Froude number normal to the wavefront
g	=	gravity acceleration
h_1	=	average water height upstream of the jump
h_2	=	water height in each measurement point downstream of the jump
h_{max}	=	wave height of the first wave crest in the undular jump in the centreline longitudinal section
L	=	longitudinal length from the upstream channel gate to the hydraulic jump front normal to the upstream current
l	=	longitudinal distance from the upstream channel gate to the toe of the shock wave
Re	=	Reynolds number
T	=	water temperature
V_0	=	averaged upstream flow velocity
V_1	=	flow velocity in measurement points upstream of the jump
V_2	=	flow velocity in measurement points downstream of the jump
V_{n1}	=	velocity normal to the wave front in each measurement point before the jump
V_{n2}	=	velocity normal to the wave front in each measurement point after the jump
V_{t1}	=	velocity tangential to the wave front in each measurement point before the jump
V_{t2}	=	velocity tangential to the wave front in each measurement point after the jump
x	=	longitudinal axes of the channel
y	=	transversal axes of the channel
z	=	vertical axes of the channel
β	=	angle of lateral shock wave to sidewall
λ	=	length of flow development
θ	=	angle of deflection of the velocity measured downstream of the jump
γ	=	water specific weight
ν	=	water kinematic viscosity

REFERENCES

- P.A. Carling, "Flow-separation berms downstream of a hydraulic jump in a bedrock channel", *Geomorphology*, (1995), 11, pp. 245-253.
- H. Chanson, J.S. Montes, "Characteristics of undular hydraulic jumps: experimental apparatus and flow patterns", *ASCE, Journal of Hydraulic Engineering* (1995), 121 (2), pp. 129-144.
- V.T. Chow, *Open Channel Hydraulics*, McGraw-Hill Book Company, New York (1959).
- A.T. Ippen, "Mechanics of supercritical flow", *Trans. ASCE* (1951), 116, pp. 268-295.
- A.T. Ippen, D.R.F. Harleman, "Verification of theory for oblique standing waves", *Transactions, ASCE* (1956), 121, pp. 678-694.
- H.J. Leutheusser, S. Alemu, "Flow separation under hydraulic jump", *IAHR, Journal of Hydraulic Research* (1979), 17 (3), pp. 193-206.
- J.S. Montes, H. Chanson, "Characteristics of undular hydraulic jumps: experiments and analysis", *ASCE, Journal of Hydraulic Engineering* (1998), Vol. 124, No. 2, pp. 192-205.
- I. Ohtsu, Y. Yasuda, H. Gotoh, "Hydraulic condition for undular-jump formations", *IAHR, Journal of Hydraulic Research* (2001), 39 (2), pp. 203-209.
- I. Ohtsu, Y. Yasuda, H. Gotoh, Discussion of "Characteristics of undular hydraulic jumps: experimental apparatus and flow patterns" by H. Chanson and J.S. Montes (Paper 7859), *ASCE, Journal of Hydraulic Engineering* (1997), 123 (2), pp. 161-164.
- I. Ohtsu, Y. Yasuda, H. Gotoh, "Flow conditions of undular hydraulic jumps in horizontal rectangular channels", *ASCE, Journal of Hydraulic Engineering* (2003), 129 (12), pp. 948-955.
- R. Reinauer, W.H. Hager, "Non-breaking undular hydraulic jumps", *IAHR, Journal of Hydraulic Research* (1995), 33 (5), pp. 1-16.

- R. Reinauer, W.H. Hager, "*Shockwave in air-water flows*", Int. J. Multiphase Flow (1996), 22 (6), pp. 1255-1263.
H. Rouse, B.V. Bhoota, E.-Y. Hsu, "*Design of channel expansions*", Trans. ASCE (1951), 116, pp. 347-363.